

Very High Energy Cosmic Rays and Their Interactions

Ralph Engel^a

^aForschungszentrum Karlsruhe, Institut für Kernphysik, 76021 Karlsruhe, Germany

The investigation of high energy cosmic rays and their interactions is a very active field of research. This article summarizes the progress made during the last years as reflected by the contributions to the XIII International Symposium on Very High Energy Cosmic Ray Interactions held in Pylos, Greece.

1. Introduction

The investigation of very high energy cosmic rays and their interactions are inherently connected subjects of astroparticle physics. On one hand the understanding of cosmic ray interactions is needed to study the flux, acceleration and propagation of cosmic rays. For example, the high energy cosmic ray flux can only be measured by linking secondary particle cascades observed in detectors or the Earth's atmosphere to primary particles of certain energy, mass number and arrival direction. Furthermore the knowledge of particle production is needed for the interpretation of secondary particle fluxes due to cosmic ray interactions in various astrophysical environments. On the other hand cosmic rays provide us with a continuous beam of high energy particles that can be exploited for studies of interaction physics at energies and phase space regions not accessible at man-made accelerators.

Cosmic ray research of the last years is characterized by substantial progress in measuring primary and secondary particle fluxes.

Examples for new results on the primary cosmic ray flux are the measurements below the knee by AMS, BESS and ATIC, in the knee energy region by KASCADE and TIBET, and at the highest energies by the High Resolution Fly's Eye (HiRes) experiment. Still some of the experimental results appear contradictory and are subject of controversial discussions. For example, the results of the composition analyses of the KASCADE and EAS-TOP data seem to be in variance with a first, preliminary analysis of the TIBET data. Similarly, there appears to be a discrep-

ancy between the AGASA measurements of the cosmic ray flux above 10^{20} eV and the new HiRes data.

In addition to the measurement of the primary cosmic ray flux the most powerful method of improving our understanding of cosmic ray physics is the study of secondary particle fluxes. New instruments measuring gamma-rays (CANGAROO, HESS, MAGIC, VERITAS, and Milagro), muons and neutrinos (AMANDA, BAIKAL, NESTOR, and ANTARES) have begun taking data or successfully performed prototype runs. Regarding cosmic ray physics, they are expected not only to test models of cosmic ray acceleration and interaction in supernova remnants and other astrophysical objects but also to provide valuable clues on cosmic ray composition and the characteristics of high energy particle production.

There are many efforts to develop better models for cosmic ray interactions or to derive information on hadronic multiparticle production. The progress in this field is closely linked to measurements of forward multiparticle production in fixed-target and collider experiments.

One of the central problems is the consistent implementation of the consequences of the steeply rising parton densities measured in deep inelastic e-p collisions at HERA and the indications of parton density saturation seen at the Relativistic Heavy Ion Collider RHIC. RHIC data clearly demonstrate the difficulties of extrapolating models tuned to accelerator data to higher energy or other projectile/target combinations. Many models predicted a secondary particle multiplicity exceeding that measured in central Au-Au collisions by $\sim 30\%$ or more. The impact of the RHIC

data on the extrapolation of cosmic ray interaction models to ultra-high energy is still far from being understood.

Measurements of cosmic ray showers and secondary particle fluxes have reached a precision that they become increasingly important in constraining hadronic interaction models. Despite providing mainly indirect information on hadronic multiparticle production they allow the exclusion of extreme model extrapolations and limit exotic physics scenarios.

This article presents a summary of recent developments in the field of very high energy cosmic ray physics and related interaction physics, focusing on the contributions presented at the XIII International Symposium on Very High Energy Cosmic Ray Interactions. The plan of the paper is as follows. In Sec. 2 the current status of cosmic ray flux measurements is given. Results of different measurements are compared and their dependence on hadronic interaction models employed for data analysis is discussed. The progress in modeling extensive air showers is outlined in Sec. 3, focussing on status and uncertainties of high-energy interaction models. Motivated by the current use of QGSJET as “standard candle” interaction model in almost all high energy cosmic ray experiments, uncertainties and features of interaction models are discussed in some detail. The importance of analyzing observables of relevance to cosmic ray physics in experiments at current and future accelerators is emphasized. Sec. 4 gives a short update on the controversial subject of exotic interaction features claimed to be found in emulsion chamber measurements. The very active field of measuring gamma-rays, muons and neutrinos produced in cosmic ray interactions is briefly touched upon in Sec. 5. Finally, conclusions and an outlook is given in Sec. 6.

2. Cosmic ray flux

For understanding very high energy cosmic rays and their sources, the measurement and interpretation of the all-particle flux, the elemental composition (including the γ -ray fraction), the arrival direction distribution (large scale anisotropy,

small scale clustering, and correlation with hypothetical sources), and temporal variations are of central importance. We will briefly discuss these topics beginning with the highest energies. Recent reviews of the experimental situation can be found in [1,2,3,4,5].

2.1. Ultra-high energy cosmic rays

At the highest energies, the Akeno Giant Air Shower Array (AGASA) and the High Resolution Fly’s Eye (HiRes) detectors are the installations with the biggest accumulated aperture that have published flux data. The flux data from both experiments are shown in Fig. 1.

First of all there is the well-known and often discussed discrepancy between the two data sets at very high energy. Whereas the AGASA data do not show any sign of the expected GZK cut-off [24] in the energy spectrum [7,25], the HiRes results are compatible with such a GZK signature [10,11]. The statistical significance of this discrepancy above 10^{20} eV is about $2-3\sigma$ [26]. At lower energy, the overall difference between the measurements is well within the range of the systematic errors of both experiments [27,28]. This also applies to the independent data set from the Yakutsk array [29] which is characterized by a larger shower-to-shower reconstruction uncertainty of 32 - 46% as compared to about 20% for HiRes and AGASA. The Yakutsk array also has an integrated aperture $\sim 40\%$ smaller than AGASA.

Secondly there is a smooth transition between the HiRes and AGASA data and the lower energy measurements of the prototype instrument HiRes-MIA [13] and the Akeno air shower array [8,9], respectively. This might indicate a systematic bias in one or both measurement techniques that could be related to the simulation of ultra-high energy air showers.

To estimate the elemental composition of ultra-high energy cosmic rays (UHECR), both AGASA and HiRes have analyzed their data in terms of a two-component proton/iron composition hypothesis.

The HiRes analysis is based on the measurement of the depth of shower maximum. Using the hadronic interaction model QGSJET [30,31]

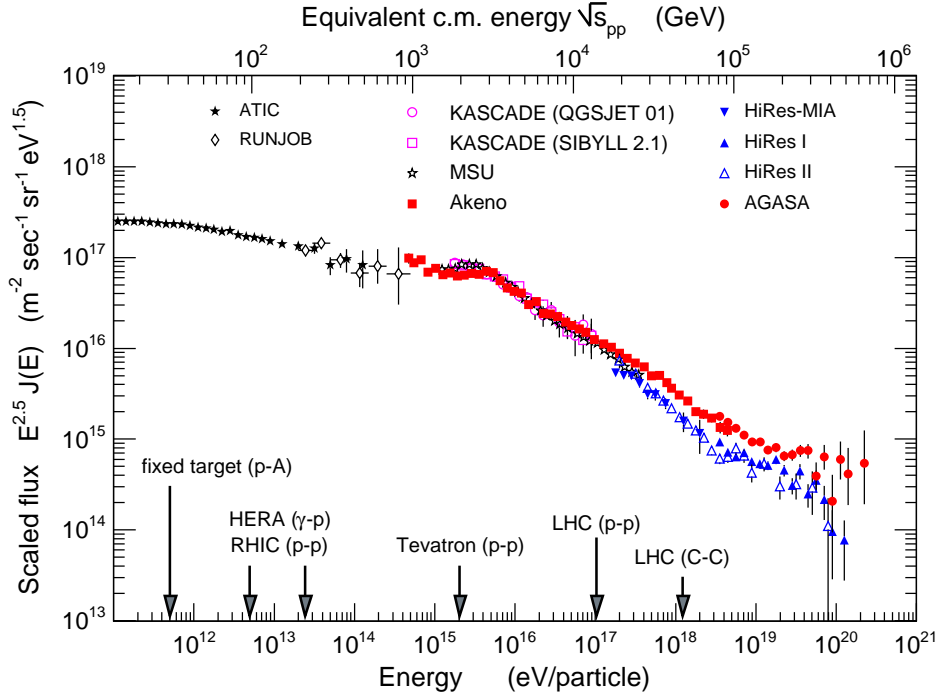


Figure 1. Primary cosmic ray flux scaled with $E^{2.5}$. Shown is a selection of recent measurements as discussed at this meeting together with some older data for reference (AGASA [6], Akeno [7,8,9], HiRes [10,11,12], HiRes-MIA [13], KASCADE [14,15], MSU [16], RUNJOB [17,18], ATIC [19]). For the sake of clarity, the all-particle fluxes from EAS-TOP [20,21] and Tibet [22,23] are not shown. They cannot be distinguished from the others in this representation.

for interpreting the data they find a transition to a light composition [13] that remains proton dominated (80% protons) between 10^{17} eV and $10^{19.3}$ eV [10,32]. Preliminary results of the re-analysis of the AGASA muon density data measured with the Akeno muon detectors show also a transition to a proton dominated composition. In contrast to the HiRes results, the transition is found to occur gradually over a large energy range. From about 50% iron fraction at $10^{17.5}$ eV the iron contribution drops below 20% at 10^{19} eV [7,33]. Similar to the HiRes analysis, the Yakutsk composition measurement [34] is related to the primary mass sensitivity of the shower depth of maximum. The Yakutsk group find a light composition of about 70-80% proton and helium in the energy range $5 \times 10^{17} - 5 \times 10^{18}$ eV [34].

The most natural interpretation of the chang-

ing composition would be the transition from Galactic to extragalactic cosmic rays. The transition energy would be somewhere between 10^{17} and 10^{19} eV. Whereas HiRes data are consistent with the interpretation that the “ankle” in the cosmic ray spectrum is already a signature of the GZK cutoff (e^+e^- -pair production of protons with photons of the CMB) [35,36], AGASA data favour an interpretation of the ankle as transition region between Galactic and extragalactic cosmic rays.

It is clear, however, that these composition measurements are strongly model dependent as there is a large theoretical uncertainty in predicting electron and muon shower sizes as well as the depth of shower maximum for hadron-induced showers [37,38,39]. An interpretation based on SIBYLL [40,41] or neXus [42] gives a heavier com-

position: about 30 and 50% iron, respectively (see also Fig. 5). It is unclear which of the model predictions is more realistic and also whether the range of predictions exhausts the range of the theoretical uncertainties (see discussion in Sec. 3). Moreover there are signs of inconsistencies [43,3]. For example, the muon densities measured for the same showers as used in the depth of maximum analysis of the HiRes-MIA data are similar to or even exceed those expected for iron primaries [13]. Furthermore investigations based on mass-sensitive observables such as shower disk thickness and shape of the lateral distribution also indicate a heavier composition ($\sim 80 - 90\%$ iron) [44,45].

Limits on the primary photon fraction were given by AGASA based on the investigation of showers with muon density information. The fraction of photon-induced showers is found to be smaller than 28% (67%) at energies greater than 10^{19} ($10^{19.5}$) eV at 95% CL. A recently developed method of comparing shower-by-shower measurements with theoretical expectations for photon-induced showers [46] allows one to derive a limit at even higher energy where the statistics is very sparse: less than 65% of all showers with energies above 1.25×10^{20} eV are initiated by photons (95% CL) [47].

Given the limited statistics accumulated until now, the arrival direction distribution of UHECR appears isotropic. There are a number of cosmic rays forming arrival direction multiplets in the AGASA data set (57 events with $E > 4 \times 10^{19}$ eV: 6 doublets, 1 triplet) [7,48]. The statistical significance of this small scale clustering is subject to controversial discussion. If the clustering were found with “a priori” chosen values for energy threshold and separation angle, i.e. without performing a scan in energy threshold and separation angle, the chance probability would be less than 10^{-4} . Assuming that such a scan was performed, the chance probability would increase to about 0.3% [49].

The exposure of HiRes in stereo mode has not yet reached that of AGASA¹. There are 27 events

detected in stereoscopic mode above 4×10^{19} eV. Using this data set in an autocorrelation analysis no significant small-scale clustering is found. Adding the HiRes stereo data set to that from AGASA only one additional pair is found. The clustering found in the combined data set is estimated to have a chance probability of 1%.

The search for correlations with astrophysical sources is hampered by the incompleteness of catalogs and related object detection and selection biases. Assuming that the source distribution follows that of the luminous matter in the universe it is natural to expect a correlation with the supergalactic plane [50]. No such correlation is found in the current data sets. There are a number of correlations claimed between the AGASA and Yakutsk data sets and BL Lacs [51,52,53]. With an angular resolution of about 0.7° , the HiRes stereo data set is ideally suited for such studies. Using the same astrophysical objects no correlation with the HiRes events is found for energies above 2.4 and 4×10^{19} eV.

Recently new indications of a correlation with BL Lacs were found if the energy threshold for comparison is lowered to 10^{19} eV (10 out of 271 showers have arrival directions within 0.8° of one of the 156 selected BL Lacs from the Veron catalog) [54]. The chance probability of finding such a correlation in an un-correlated data set is estimated as 0.1%, but only a new, independent data set will allow to assess the significance unambiguously. Taken at face value, the correlation would have to be interpreted as a small fraction of neutral particles in UHECR.

Currently there are two large-aperture detectors for UHECR in construction, the Pierre Auger Observatory [55,56] and the Telescope Array (TA) [57,58]. Both detector concepts employ the hybrid detection technique of measuring air showers with surface detectors (Auger: water Cherenkov tanks, TA: plastic scintillators) and fluorescence telescopes. The hybrid technique will allow a good energy calibration of showers measured with surface detectors and improve the ability of composition measurements.

¹Viewing showers in monoscopic mode HiRes I has reached a higher accumulated aperture than AGASA for energies above 3×10^{19} eV. However, due to the limited and highly

asymmetric angular resolution, the HiRes I mono data set is not suited for studying small scale clustering.

After testing the detector design with an engineering array [59] the construction of the southern Auger observatory in Malargue, Argentina is in full progress [55]. At the time of writing this article about 800 of the planned 1600 surface detector stations and 50% of the fluorescence telescopes are completed. Already during the construction phase the integrated aperture of Auger has reached that of 10 years of data taking with AGASA. It is planned to build a similar observatory in the northern hemisphere to obtain nearly uniform full sky coverage.

2.2. Knee energy region

In contrast to previous measurements in the knee energy region (for example, see the compilations in [60,2,61]) the recent all-particle flux measurements by KASCADE [14], EAS-TOP [20], and Tibet [23] agree within 10% with each other. The knee is at about 3×10^{15} eV and no deviation from a broken power law with a smooth transition region is found within the current experimental resolution.

Concerning the elemental composition, the situation is less clear. There is increasing evidence for a transition from a mixed to a heavy composition with increasing energy. However, the detailed change of composition through the knee energy range is still unclear.

All experimental results discussed at the meeting show a trend towards a heavy composition with increasing energy (KASCADE [14], Tibet [22], EAS-TOP [20], and SPASE/AMANDA [62]). However, it is difficult to find observables that demonstrate this transition beyond doubt as all composition studies depend very much on the hadronic interaction models used for data interpretation and alternative explanations might be possible, although unlikely (see, for example, [63]). Probably the least model dependent analysis is that of muon-rich and muon-poor showers by the KASCADE Collab. [64], which demonstrates that the knee is mainly caused by a disappearance of the light (i.e. muon-poor) flux components.

The high-statistics data of multi-detector setup KASCADE [65] allow the analysis of the correlated muon ($E_\mu > 240$ MeV) and electron sizes

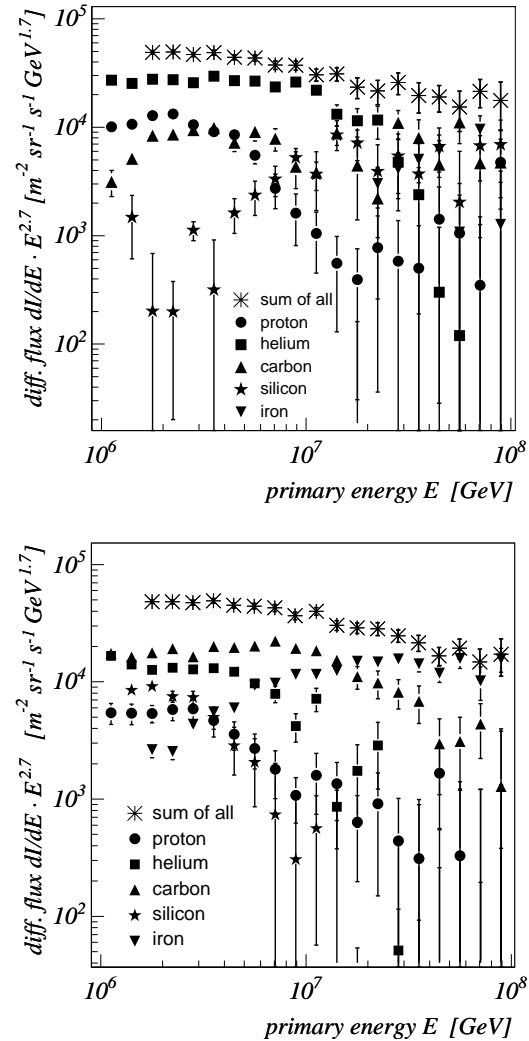


Figure 2. Flux derived for 5 elemental groups from KASCADE data [14,15]. The top panel shows the results obtained with QGSJET 01, the bottom panel those with SIBYLL 2.1.

of showers in terms of 5 mass groups [14,15]. Fig. 2 shows the results for two hadronic interaction models, QGSJET and SIBYLL. In this analysis, the derived all-particle flux turns out to be almost independent of the used hadronic interaction model. However, the different elemental fluxes vary strongly. For example, using QGSJET

the flux appears dominated by helium below the knee with no significant iron contribution. The SIBYLL-based interpretation favours instead helium and carbon below the knee and a small but significant fraction of iron primaries is needed. Both models do not provide a fully consistent description of the KASCADE N_e - N_μ data. The found deviations underline the high statistical accuracy of the KASCADE data and show the need of improving hadronic interaction models.

The interpretation of the KASCADE data with both models shows that the flux of the light components exhibits a break in the power law at different energies with lighter elements having a lower break energy. No spectral break is found for iron in the considered energy range. One of the central questions is that of the scaling of the break energies. Acceleration and propagation models for the knee typically predict rigidity-dependent scaling whereas models with new particle physics lead to mass-dependent scaling. Unfortunately, the strong had. interaction model dependence does not allow us to draw conclusions on a possible mass- or rigidity-dependent scaling of the break energies.

The composition measurement by the EAS-TOP Collab. [20,21] is based on 3 elemental groups and uses electron and GeV-muon data. It shows the same qualitative behaviour of the elemental groups as seen in the KASCADE analysis. The iron-like mass group does not exhibit a break in the power spectrum and seems to have a harder power law index than the light component. The knee appears to be caused by elements in the mass range of proton and helium with a break energy of about 3.5×10^{15} eV.

Some of the air showers measured with the EAS-TOP and SPASE arrays produce high-energy muon bundles that can be detected with MACRO ($E_\mu > 1.3$ TeV) and AMANDA ($E_\mu > 300$ GeV), respectively. Again, analyses of the coincidence data sets show a transition from a mixed to a heavy composition [20,66,62,67].

The preliminary and statistically limited measurement of the proton flux by the Tibet AS γ Collab. [68] seems to be at variance with KASCADE and EAS-TOP results. Over the energy range from 2×10^{14} to 10^{16} eV the proton spec-

trum is found to follow a power law with the index 3.14 ± 0.10 . By comparing the Tibet proton spectrum with that of RUNJOB and JACEE a much lower break energy of $\sim 5 \times 10^{14}$ eV is inferred.

The reasons for the discrepancy between Tibet and KASCADE/EAS-TOP data is not yet understood. However, it should be noted that both KASCADE and EAS-TOP employ in their analysis the electron-muon size correlations in showers whereas the Tibet measurement is based on a neural net analysis of a number of shower observables that combine emulsion chamber information with scintillator data: N_γ (multiplicity of a family), $\sum E_\gamma$ (energy sum of a family), $\langle R_\gamma \rangle$ (mean lateral spread of a family), $\langle E_\gamma \cdot R_\gamma \rangle$ (mean lateral spread of the family energy), and N_e (shower size) [68]. Furthermore all three experiments are at different altitudes and probe different stages of shower evolution. Tibet is at a vertical depth of 606 g/cm², EAS-TOP at 820 g/cm² and KASCADE at 1020 g/cm². The use of different air shower simulations can be ruled out as all experiments now apply CORSIKA [69].

Due to the large statistical errors, the direct flux measurements of individual mass groups by JACEE [70], RUNJOB [17,18] and ATIC [71] do not yet impose strong constraints on the air shower data. All composition data discussed here are compatible with possible extrapolations of direct measurements at lower energy.

In cosmic ray models that explain the knee by propagation effects (leakage from our Galaxy), an increasing dipole anisotropy of the shower arrival directions is expected (i.e. [72]). Analyzing 2×10^7 showers in the knee energy range the KASCADE group do not find any significant anisotropy signal [73]. Similarly, no cosmic ray point sources are seen [74].

Being located at higher altitude, the Tibet array has a much lower energy threshold. Again, no Galactic anisotropy was found in the Tibet AS γ data. However, using more than 5×10^9 showers with $E > 3 \times 10^{12}$ eV, the Tibet AS γ Collab. could detect the dipole anisotropy due to the orbital motion of the Earth around the Sun (Compton-Getting effect) with an amplitude of about 0.1% [22,75] (see also [76]).

3. Modeling of cosmic ray interactions and EAS

Given the dependence of the cosmic ray flux and composition measurements on the understanding and modeling of hadronic interactions of cosmic rays and their secondary particles, it is natural to assume that discrepant results discussed in the previous section can be, at least to some extent, traced back to the use of different models for data interpretation.

Several groups have shown that an analysis of the same data set with different hadronic interaction models can lead to a wide range of different results (see, for example, [21,15]). This means that the use of the same shower simulation model is pre-requisite for a fair comparison of the results of different experiments.

Another important aspect of inter-experiment comparison is the use of sufficiently realistic and accurate shower simulations. For example, using the same model for shower evolution, one can obtain different interpretations of the data if different observables of the showers are considered [77]. Therefore experiments might arrive at contradicting conclusions even if the same shower simulation tools are used.

The largest uncertainty in EAS simulation stems from the unknown characteristics of hadronic multiparticle production [78,79]. As has been realized during the last years, also interactions at intermediate energies can contribute significantly to this uncertainty, though to a smaller extent [80,81,82]. In addition there are uncertainties coming from the treatment of electromagnetic interactions and differences in details of particle transport and decay implementations [79].

Motivated by different models of hadronic multiparticle production, three energy regions are distinguished. At very low energy (close to the particle production threshold up to a few GeV) particle production is characterized by the production and decay of resonances. Knowing all resonances and their decay branching ratios allows one to construct a rather complete model for the interaction cross section and hadronic final states. For example, the codes HADRIN [83] and SOPHIA [84] have many resonance chan-

nels tabulated. The intermediate energy range up to about 10^3 GeV can be well understood in a model that describes particle production on the basis of the fragmentation of two color strings (i.e. older versions of FLUKA [85]). At energies above 10^3 GeV minijet production and multiple parton-parton interactions become important and require again a different modeling. The most frequently used high energy models are DPMJET [86], neXus [42], QGSJET [31], and SIBYLL [40].

In the following we will summarize some important recent developments in modeling hadronic interactions and related activities of measuring hadron production in accelerator experiments, and will discuss new trends in air shower simulation.

3.1. Hadronic interactions at high energy

There are basically four central assumptions that characterize a model's high energy extrapolation [88,89,90]:

- (i) size and energy dependence of the QCD minijet cross section,
- (ii) distribution of partons in transverse space (profile function),
- (iii) scaling of leading particle distributions or scaling violation, and
- (iv) treatment of nuclear effects (semi-superposition model, Gribov-Glauber approximation, increased parton shadowing, etc.)

It is beyond the scope of this article to discuss all models and their differences. We shall concentrate here on aspects relevant to p-air interactions and consider only the two most frequently applied models, QGSJET and SIBYLL. Apart from the treatment of nucleus-nucleus collisions, QGSJET and SIBYLL differ mainly in the first two points [91,89].

Since version 2.1, "post-HERA" parton densities are used in SIBYLL for calculating the minijet cross section whereas QGSJET 01 (and the earlier version QGSJET 98) was developed with older, "pre-HERA" parton densities. Another

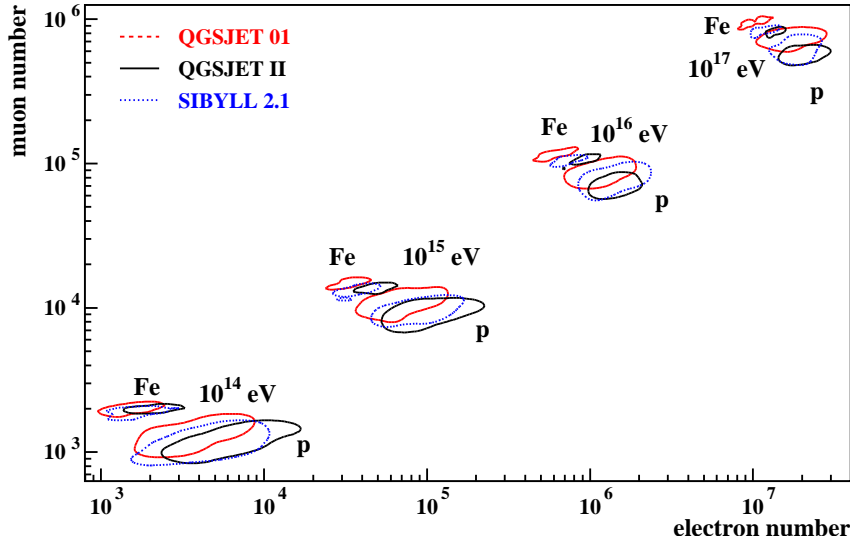


Figure 3. Electron-muon size correlation for showers simulated with CORSIKA [87]. Predictions of the old and new versions of QGSJET [38] are compared with SIBYLL 2.1 [41].

important difference between the models is the treatment of the minijet transverse momentum cutoff needed to restrict the minijet calculation to the perturbative QCD domain. In QGSJET 01 an energy-independent, constant value of 2 GeV is used. The SIBYLL authors implemented an energy-dependent transverse momentum cutoff whose value is similar to that of QGSJET 01 at low energy but increases to about 8 GeV at 10^{20} eV [41]. This was needed as “post-HERA” parton density functions predict at ultra-high energy gluon densities that lead to overlap of individual gluon wave functions in a proton for a transverse momentum cutoff as low as 1.5 GeV (see [92], a recent review on this subject is [93]). In this phase space region non-linear evolution equations have to be used to describe parton densities. The expected size of the non-linear corrections is theoretically not understood and subject of intense research [94]. There are models that predict an early and total saturation of the gluon density (color glass condensate [95]) and others with moderate changes.

Many experiments are searching for signs of deviations from linear parton density evolution equations or gluon density saturation. Although

HERA and RHIC are colliders with CMS energies of $\sqrt{s} \sim 200$ GeV, corresponding to only 2×10^{13} eV, they are currently the best instruments for studying saturation effects. At HERA, parton densities of quarks are measured directly and, through scaling violations, that of gluons derived. HERA data can be described assuming parton density saturation, for example, in terms of the Golec-Biernat–Wüsthoff model [96], or applying perturbative QCD without any non-linear effects [97,98]. At RHIC, parton densities cannot be measured directly. However, the scaling of jet rates and other observables with the number of participating nucleons depends on the assumptions on the number of partons in the very gluon-dense environment of a heavy nucleus. Many aspects of RHIC data indicate strong deviations from naive parton model predictions [99,100] but the energy range of the collisions is too limited to show unambiguously that the effects observed so far are requiring parton density saturation [101].

The problem of using “post-HERA” parton densities for extrapolating hadronic interactions to ultra-high energy $\sqrt{s} \sim 500$ TeV within the Quark-Gluon Strings Model [102] is addressed in the new version of QGSJET, called QGSJET-

II [103]. Different from the SIBYLL approach, the transverse momentum cutoff is kept energy-independent. This is achieved by introducing non-linear effects for partons below the perturbative scale, equivalent to non-linear evolution equations. As one cannot speak of individual partons in the soft, non-perturbative domain, these non-linear effects are implemented as multi-pomeron interactions (enhanced pomeron graphs [104]), which are summed to all orders. Other important improvements are the treatment of diffraction dissociation. Whereas the old version of QGSJET had a fixed ratio of diffractive to elastic cross sections (grey disk limit, see also [105]), the new version approaches at high energy the black disk limit (see discussion in [88]). Furthermore QGSJET-II was tuned to better describe the secondary particle multiplicity at low collision energy. Although the latter changes are more of technical nature they still are important. The old version predicted at low energy too high a pion multiplicity, a possible reason for higher GeV-muon multiplicities obtained for EAS than found with other models [106,82]. It is clear that QGSJET-II is a much more theoretically consistent model than the previous versions.

There are a number of important consequences from these changes in QGSJET. First of all the low- x extrapolation of the parton densities becomes less steep than naively expected in linear perturbative QCD. Secondly there are changes of the effective parton densities acting in hadron-hadron collisions in dependence of the projectile and target mass number A (suppression for large A). This leads to the violation of the superposition approximation even for fully inclusive observables.² Thirdly the fluctuations in inelasticity are considerably reduced. The leading particle distributions are now qualitatively similar to those of SIBYLL and DPMJET [107].

The impact of the QGSJET improvements on air shower predictions is currently under investigation [107]. For example, Fig. 3 shows the electron-muon size correlation for vertical EAS

at sea level [87]. The contours are iso-lines of the correlation function at half maximum. For a given energy the number of muons is reduced significantly. At the same time 30-40% more electrons are expected at detector level in the knee energy region. The interpretation of data from experiments that utilize electron and muon numbers as composition sensitive observable (e.g. KASCADE, EAS-TOP) will change towards a heavier composition if QGSJET-II is used.

At the highest energies, the predictions of the electron numbers of the old and new QGSJET versions are not very different. Still it can be expected that the energy calibration of experiments like AGASA would have to be revised downward though detailed simulations are needed to estimate by what amount. Experiments like Auger [55] will be much more sensitive to the modifications: the predicted muon density at 600 to 1000 m from the shower core is reduced by $\sim 30\%$. Using QGSJET-II also the interpretation of fluorescence measurements will change and shift towards a heavier composition as the mean depth of maximum is increased by 10 g/cm^2 and 20 g/cm^2 at 10^{20} eV for proton and iron showers, respectively [38].

Different assumptions on the QCD minijet cross section, i.e. calculated with or without saturation, lead to enormous differences in the model extrapolations [88]. The most striking example is the secondary particle multiplicity in p-air collisions. At ultra-high energy, QGSJET 01 predicts a more than 3 times higher secondary particle multiplicity than SIBYLL [78,89]. Due to the implementation of new parton densities, the multiplicity of QGSJET-II is even higher than that of QGSJET 01 at ultra-high energy. However, these differences are of very much reduced importance for the evolution of air showers as most of the secondary particles have a very small energy. Of greater importance are two model characteristics that are indirectly linked to the minijet cross section: the total p-air and π -air cross sections and the distribution of leading secondary particles.

The total cross section of a model depends at high energy mainly on the minijet cross section and the transverse profile function which is a measure of how partons are distributed in a hadron

²In the simplest version of the superposition model, an iron-induced shower is equivalent to 56 proton induced showers having 1/56 of the shower energy. The superposition model is expected to be valid for inclusive observables.

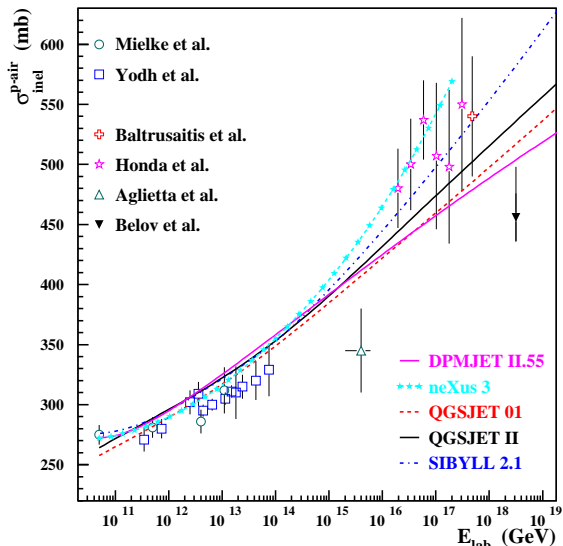


Figure 4. Compilation of p-air production cross sections and model predictions (from [79], modified and updated [107]).

[89]. It is the difference of the assumed profile functions and minijet cross sections and the lack of data to distinguish between these assumptions that lead to widely varying high-energy cross section extrapolations (see Fig. 4). Cross section measurements over a wide range of energy would help to reduce the model ambiguities. Although hadron-air cross sections are needed for simulation, p-p and p- \bar{p} cross section measurements are also of great interest. Using the Gribov-Glauber approximation, cross sections with air can be estimated using nucleon-nucleon cross section data. At the moment, due to the contradicting total p- \bar{p} cross section measurements at Tevatron [108,109], possible theoretical extrapolations are experimentally not very much restricted [88,110]. Therefore the planned total cross section measurement with the TOTEM/CMS detector combination at the LHC [111,112], corresponding to an equivalent energy of about 10^{17} eV, will be of outstanding importance.

All current high energy interaction models are based on the implicit assumption that leading particle distributions scale with energy. The lead-

ing particle distributions are tuned to low-energy data and change at high energy only due to energy-momentum conservation effects as the energy has to be shared between the leading particles and the increasing bulk of low-energy secondary particles. This assumption seems to describe the very sparse data we have on leading particle production up to HERA energy ($\sim 2 \times 10^{13}$ eV) [113]. However, there are theoretical arguments that the leading particle distributions will change drastically at ultra-high energy [114].

If parton density saturation indeed occurs at cosmic ray energies, a collision can be viewed as black disk scattering: the gluons completely “fill” the target nucleus [37,115,116]. Not only the very numerous partons at small x but also the much faster valence quarks will participate in the interaction. Indeed, in a non-peripheral collision (complete saturation) the chance probability of valence quarks to scatter off these gluons approaches unity. As a consequence this will lead to the disintegration of the leading valence di-quark: no leading baryon is produced and the elasticity of the collision drops by almost a factor 2.

Indeed there are some indications of “anomalous” baryon stopping in heavy ion collisions, however, at much lower energy (for example, [117, 118]) and different theoretical interpretations are put forward (for example, string junction interpretation: [119,120] and saturation [121]). Measurements of hadron production in the very forward direction at RHIC [99], Tevatron [108], and LHC [111] will be needed to study the leading baryon distributions systematically and clarify the situation.

The implementation of different scenarios of parton density saturation in the SIBYLL 2.1 code allows a first estimate of the expected effects and their dependence on model parameters [115,116]. In a conservative scenario the mean depth of shower maximum, $\langle X_{\text{max}} \rangle$, is reduced by about 20 g/cm^2 at 10^{19} eV, corresponding to the difference between SIBYLL and QGSJET 01 predictions. Depending on the assumptions, much larger reductions of $\langle X_{\text{max}} \rangle$ are possible.

3.2. Hadronic interactions at intermediate energy

Hadronic interactions in air showers at intermediate energy are often simulated with models like GHEISHA [122] (used in CORSIKA [69]) or the Hillas splitting algorithm [123] (used in MOCCA [124] and AIRES [125]). Both models are very fast but rather crude parametrizations of low-energy data or interaction physics. Their application is certainly justified if only the electron/photon component of a shower or calorimetric quantities are studied as in this case the details of low-energy interactions are of minor importance.

The situation is, however, different for muons. Due to successive hadronic interactions, the number of pions and kaons increases in an air shower with decreasing particle energy. Below some 100 (500) GeV pions (kaons) are more likely to decay than to undergo further interactions. Therefore, hadronic interactions in the energy range from several GeV to a few hundred GeV are very important for understanding GeV muon production in EAS of all energies [80,81]. Recent studies have shown that the muon density at large lateral distance is indeed very sensitive to the model used for low- and intermediate-energy interactions. The differences between the predictions of the various models are of the order of 10-20% in the relevant lateral distance range but can be as large as 50% [126,82].

A detailed comparison of low- and intermediate-energy models to available data [82,127] show that GHEISHA does not provide an adequate parametrization of the interaction characteristics. The Hillas splitting algorithm seems to give a somewhat better description but a thorough comparison to data is hampered by the limitation to only p/ π -air collisions. The best models available are clearly FLUKA [85] and UrQMD [128] but there are still significant differences between the predictions of these two models.

The energy range up to 400 GeV is in reach of fixed-target accelerator experiments. Not only that such experiments can easily measure with light, air-like nuclei as targets they can also run with tagged pion and kaon beams and measure

particle production in the very forward direction. Recognizing the importance of low-energy measurements for atmospheric neutrino flux predictions [129] and neutrino factories, a programme was begun to systematically measure pion and kaon production in minimum bias collisions. Examples are the HARP experiment [130,131] where first data are available now, the NA49 minimum bias p-C run [130], and the MIPP experiment [108,132] which is currently taking data.

3.3. Information from air shower measurements

It is difficult to obtain information on hadronic multiparticle production at ultra-high energy from EAS measurements. First of all the primary particle mass is, in general, not known. Secondly, the large number of successive hadronic interactions smears out any striking features of the primary interaction. Therefore most analyses of air shower data in terms of interaction physics are highly indirect and often serve only the exclusion of extreme scenarios (for example, [37]).

One of the most interesting measurements of this kind is the analysis of deeply penetrating air showers to obtain the inelastic proton-air cross section. Traditionally an exponential function is fitted to the observed X_{\max} distribution and the derived absorption length Λ is converted to the interaction length via a so-called k -factor (for a recent discussion, see [133]). The HiRes Collab. developed a new method that does partially avoid the ambiguities of the definition of a k -factor [134]. Applying this method to the stereo data set, a preliminary p-air cross section of $456 \pm 17(\text{stat}) + 39 - 11(\text{sys})\text{mb}$ at $10^{18.5}\text{eV}$ is derived [135]. This cross section is lower than the current model extrapolations, see Fig. 4. A number of possible biases still need to be investigated. For example, a small fraction of photon primaries would be enough to spoil the cross section measurement as photon-initiated showers have a much larger depth of maximum. Furthermore the self-consistency of the method should be checked by applying it to a model that is modified to match the actually measured cross section.

Experiments that measure many observables of air showers simultaneously can check the con-

sistency of EAS simulation. For example, the KASCADE installation allows the measurement of shower size (electrons), muon densities with thresholds of 240, 490, and 2400 MeV, and hadron multiplicities and energies above 70 GeV in the shower core [14,136]. The correlation between the different observables provides constraints on interaction models even if the full range of possible primary particles is considered [137]. The latest versions of the had. interaction models available in CORSIKA satisfy these constraints but some earlier versions are clearly at variance with the data.

Emulsion chamber experiments at high altitude have the advantage that they have a low shower energy threshold, reaching into the region of direct primary flux measurements. Therefore they are well suited for testing shower simulation models. For example, by comparing the predicted and measured optical density distribution (i.e. the energy distribution of particles in the TeV range) in emulsions of the Pamir experiment, it was found that some old versions of hadronic interaction models could be excluded [138,139].

Finally it should be noted that there are some indications of a systematic discrepancy between the mass composition derived from $N_e - N_\mu$ based measurements and that from data sensitive to the depth of maximum [140,141]. It is unclear to what extent these discrepancies are related to shortcomings in the simulation of hadronic interactions, but one can try to bring different measurements into better agreement by modifying the underlying shower simulation correspondingly. A hadronic interaction model with small cross section and a somewhat reduced inelasticity as compared to QGSJET 01 is favoured in this analysis [141].

3.4. Trends in EAS simulation

There is a lack of statistics of Monte Carlo simulations in many comparisons of data with theoretical predictions. For example, the statistics of the KASCADE shower data exceed the simulated one available for each interaction model combination by about a factor 10. A similar disparity of data to simulation statistics is also typical for modern large-scale detectors such as Auger. The

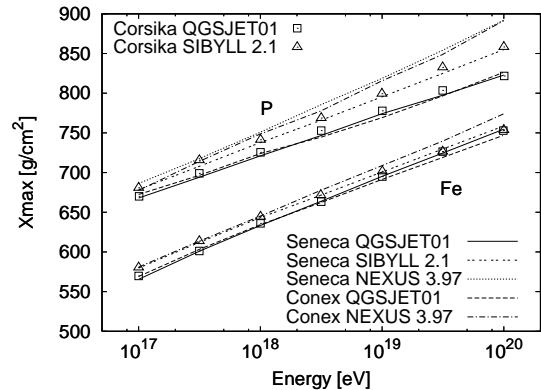


Figure 5. Mean depth of shower maximum for proton- and iron-induced showers [142]. The predictions of different hadronic interaction models as calculated with different shower codes are compared.

problem is even amplified if many observables are used to characterize each shower: the set of simulated showers should by far exceed the number of observed showers to keep the statistical reconstruction errors small.

At ultra-high energy, hybrid simulation schemes present a fast and efficient alternative to conventional Monte Carlo simulation techniques. In a hybrid simulation all interactions above a certain energy threshold are simulated with the Monte Carlo technique. Secondary particles that fall below this threshold are taken as sources of subshowers that are treated numerically. The various hybrid schemes available – for a review see [142] – differ mainly in the method of calculating these sub-showers. For example, the sub-showers could be drawn from pre-calculated libraries [89], calculated by solving cascade equations for a Monte Carlo-generated source function [39], or treated by applying numerical solutions of cascade equations together with analytical approximations or tables of shower evolution [143,144,145].

The hybrid codes SENECA [145] and CONEX [39] have several interaction models implemented and have reached a precision and sophistication that makes them suited for analyzing experi-

mental data [146]. SENECA allows a full 3+1-dimensional simulation of EAS whereas CONEX is currently restricted to calculating the projection along the shower axis. Both codes have been extensively compared to CORSIKA. For example, a comparison of the mean depth of maximum of different models is shown in Fig. 5. The agreement between the different shower simulation codes is excellent. It should also be noted that, only with hybrid simulation codes, showers can be simulated in large numbers using the time-consuming interaction model neXus 3.97 [147].

The simulation of inclined or even upward-going air showers has become increasingly important. Large-aperture experiments like Auger and EUSO have not only a large sensitivity to nearly horizontal showers but also hope to find neutrino-induced upward-going showers [55,148]. With the exception of CONEX, the currently available shower simulation packages are not optimized for such calculations. Modifications and extensions will be needed to allow detailed and efficient simulation of showers at these particularly interesting geometries.

4. Exotic phenomena and emulsion chamber data

The most striking, unexpected phenomena observed in emulsion chamber experiments are Centauro events with an exceptionally small number of photons, events with particles or groups of particles being aligned along a straight line, halo events characterized by an unusually large area of darkness in the X-ray film, and deeply penetrating cascades [149,150]. Whether these phenomena are related to fluctuations and the measurement technique of emulsion chamber experiments or signs of new physics is controversially debated for more than 30 years. In the following we will briefly discuss Centauro events and comment on the status of searching for events with alignment (see [151] for a complete review).

There are several aspects that complicate the interpretation of emulsion chamber measurements. First of all, many of these phenomena are observed only in very high energy events with estimated energy greater than 10^{16} eV, of which

only a small number of about 100 event has been collected [150]. Secondly, due to the threshold effect of the detectors ($E_\gamma > 1$ TeV), mainly proton initiated events are detected [138]. As is well known, proton showers are characterized by very large shower-to-shower fluctuations (see, for example, [152]). Thirdly, the number of high energy γ -rays and hadrons cannot be measured directly – it is obtained by comparing the tracks at various depths in the detector stacks.

Probably the most famous exotic emulsion chamber event is Centauro-I, an event with about 40 high-energy hadronic jets and only one low-energy e.m. cluster [149], see Fig. 6. Detected in 1972 in the Chacaltaya emulsion chamber experiment [153] it represents the most extreme Centauro event ever observed. In total there are about 10 Centauro events observed by the Chacaltaya and Pamir experiments (see [150], a detailed review of all events is given in [154]). No events of this kind were found in the experiments at Mount Fuji and Mount Kanbala. Also all searches at accelerators were negative.

Models proposed for explaining Centauro events range from assuming a small fraction of exotic primary particles in the cosmic ray flux (for example, strangelets [155,156] or quark globs [157]) over exotic interaction scenarios, like the creation of a disoriented chiral condensate [158] or production of evaporating mini black holes by neutrino primaries [159,160], to conventional features of diffraction dissociation [161].

Given these ongoing attempts of explaining Centauro events, the results of the recent re-examination of the emulsion chamber plates are of outstanding importance [151,162]. As it turned out, the tracks in the two chambers that were previously thought to belong to the Centauro-I event are actually due to two different events. The azimuth angle of the tracks in the upper chamber does not match that in the lower one. As there is no counterpart found in the upper chamber, this event is still very difficult to understand [162]. The probability of particles produced in an interaction well above the installation passing through a gap between the upper chambers seems to be very small. A point-like interaction in the upper layers or the wooden support frame is also un-

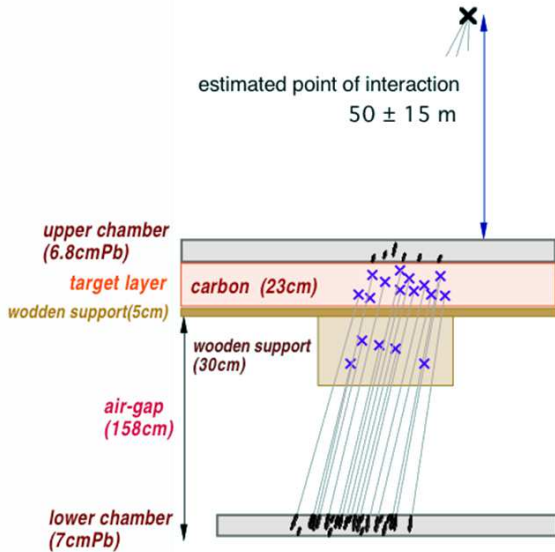


Figure 6. Illustration of the original interpretation of the Centauro-I event [151].

likely: the tracks would then correspond to very high p_{\perp} particles and should point back to the interaction vertex. No such geometric convergence of the tracks is found. This means that many particles of almost parallel trajectories have hit the emulsion chamber without interacting in the upper lead stack, again a very exotic scenario that lacks explanation.

The situation is similarly controversial regarding the experimental information on events with co-planar particle emission.

The Pamir Collab. find an excess of events with alignment of the substructures for $E > 8 - 10 \times 10^{15}$ eV [163,164]. The highest energy event measured with an emulsion experiment during a series of Concorde flights (average atm. depth ~ 100 g/cm²) shows also impressive alignment [165]. At lower energy, no excess of coplanar particle production is found. For example, measurements in the energy range below 10^{14} eV by the RUNJOB Collab. [166] and also a direct search with the CERN NA22 experiment at 2.5×10^{11} eV [164] provided distributions that agreed with the expectations. Furthermore, a recent study of

the KASCADE Collab. [167] showed that aligned structures in hadronic shower cores at sea level are not related to angular correlations in hadronic interactions as might be expected from jet production [168]. Indeed the fraction of events with alignment is only determined by the lateral distribution of hadrons. Measured in terms of the alignment parameter λ_4 , the event distributions of Pamir and KASCADE data look also surprisingly similar.

5. Gamma-ray, neutrino, and muon flux measurements

Secondary particle fluxes such as hadronically produced gamma-rays and neutrinos provide information on acceleration, propagation and interaction of cosmic rays that are complementary to what can be directly deduced from the locally observed cosmic ray flux [169,170,171]. In particular, gamma-rays and neutrinos propagate on straight trajectories, allowing the identification of the source objects or environments.

5.1. Gamma-rays

With the begin of routine operation of the second generation imaging atmospheric Cherenkov telescopes (IACT) CANGAROO [172], HESS [173,174], MAGIC [175,176], and VERITAS [177], many new TeV gamma-ray sources are discovered and their spectra measured. It is impossible to summarize the progress in this extremely active and diverse field of research and any comments made here will be soon outdated.

At the time of writing this article all big four IACT installations are completed and take data. Whereas CANGAROO and HESS have already several telescopes online, MAGIC and VERITAS work with single, but bigger telescopes. Both the MAGIC and VERITAS Collaborations are in the process of adding another telescope for stereoscopic observation with greatly improved background rejection. The HESS telescope system is characterized by an unprecedented angular resolution of 0.06° . The MAGIC telescope has a lightweight design for very fast slew to observe transient sources. It's low-energy threshold is planned

to be about 20 GeV as compared to ~ 70 GeV for HESS and VERITAS [175]. The four telescopes together give almost uniform full-sky coverage.

Highlights of the early HESS data taking are certainly the measurement of the gamma-ray flux from the Galactic Center [178] and the first observation of a SNR as spatially resolved TeV gamma-ray source (RXJ 1713-3946, a possible site of cosmic ray acceleration) [179]. Both sources were previously detected with the CANGAROO telescopes [180,181] but with much more limited resolution. The potential of the HESS telescopes is also underlined by the serendipitous discovery of an unknown TeV gamma-ray source, now called TeV J1303-63, in the field of view of the binary pulsar system PSR B1259-630 [173].

In contrast to imaging Cherenkov telescopes, air shower arrays can be used to continuously monitor the gamma-ray sky with very high duty cycle and wide field of view. The two currently operated installations of this type are Tibet AS γ [22,182] and Milagro [183,184] being located at an altitude of 4300 m and 2350 m, respectively. Whereas the Milagro Collab. employ an active hadron/gamma-ray separation via two layers of PMTs in an 8 m deep water pond, the Tibet experiment searches for arrival direction anisotropies due to gamma-rays on top of the isotropic cosmic ray background with a dense scintillator array.

Both experiments have detected the Crab SNR and the active galaxy Mrk 421 at the 5σ level [185,186]. New results from Milagro are the detection of TeV gamma-rays from the entire inner Galactic plane region and the observation of two extended sources, one coincident with EGRET source 3EG J0520+2556 and another one in the Cygnus region of the Galactic plane [187,188]. It is intriguing that the latter source coincides within the Milagro resolution of about 2° with the HEGRA source TeV J2032+4131 [189] and the region from where AGASA reported an excess of $\sim 10^{18}$ eV cosmic rays [190]. At the moment an interpretation of these observations in terms of a very high energy cosmic ray source (region) is too speculative – more data will be needed.

5.2. High-energy neutrinos

The interpretation of gamma-ray fluxes from potential cosmic ray sources suffers from ambiguities due to the superposition of different gamma-ray production processes: π^0 decay, inverse Compton scattering, synchrotron radiation, and bremsstrahlung. These uncertainties are expected to be much smaller for neutrinos as they are mainly produced in hadronic interactions via the decay of pions and kaons. Furthermore neutrinos can travel over large distances virtually unattenuated and are, therefore, ideal messenger particles, allowing a multitude of astrophysical investigations [191]. On the other hand, their small interaction cross section requires very large effective detector volumes.

There are two neutrino telescopes taking data at the moment, AMANDA-II [62,192] and Baikal NT-200 [193,194]. Although limited by detector size, the sensitivity of both detectors will approach the cascade bound in the next years³, i.e. touch the region where one can hope for a discovery. The Waxman-Bahcall bound [196] (see also discussion in [197]), often considered as a reference flux that is guaranteed if protons are the ultra-high energy cosmic rays, cannot be reached with these installations. About 3300 (370) neutrino candidates are found in the AMANDA (Baikal) data taken until end of 2003. The number of neutrinos and their distribution are compatible with the expectation from atmospheric neutrino production – neither a diffuse flux of extra-terrestrial neutrinos nor astrophysical point sources have yet been discovered.

The construction of the successor to AMANDA and much bigger neutrino telescope IceCube is on track [198]. IceCube will have a sensitivity that reaches well into the region below the Waxman-Bahcall bound, promising discoveries and many astrophysical and particle physics applications [199]. The first IceCube string was successfully deployed in February 2004 [198].

The Mediterranean neutrino telescope collaborations (ANTARES [200], NESTOR [201],

³The cascade bound, also called gamma-ray bound, is based on the assumption that all observed extragalactic gamma-rays were produced together with neutrinos in hadronic cascades [171,195].

NEMO [202]) [193] have performed prototype installations and test runs. In 2003 the ANTARES Collab. operated a prototype sector line with PMTs and a mini instrumentation line at the selected ANTARES site near Toulon (2500m water depth). Valuable information on the performance of cables and connectors under the harsh deep-sea conditions were gathered. It is planned to build the complete ANTARES detector of 12 strings and in total 900 PMTs in 2005 – 2007. NEMO has selected a site close to Sicily with nearly perfect conditions at 3500m water depth which is continuously monitored. The project is in the advanced R&D stage with the plan to build a prototype in 2005. The NESTOR site provides a large plateau at the sea floor at about 4000 m water depth. In 2003 one fully equipped prototype “star” of 32 m diameter of a NESTOR tower was successfully operated, allowing the measurement of the atmospheric muon flux. It is planned to install 7 complete towers by the end of 2006, providing a detector of about 0.15 km^3 .

It is clear that a km^3 -sized neutrino detector is needed in the northern hemisphere to complement the field of view of IceCube. Therefore the Mediterranean neutrino telescope collaborations have recently joined their efforts to construct such a detector by initiating the design study KM3NeT [203].

To measure neutrino fluxes at even higher energy, radio emission of neutrino-induced showers in dense materials can be employed [204]. Several experiments have recently performed measurements and derived first limits on the neutrino flux at ultra-high energy (FORTE [205], GLUE [206], ANITA [207]). For example, ANITA is designed to search for neutrinos with $E_\nu > 3 \times 10^{18} \text{ eV}$ by monitoring radio signals from the antarctic ice cap using a balloon-born system of antennas [204,207]. A preparatory test flight with a prototype instrument (ANITA-lite) was performed during the 03/04 austral season [204]. Already on the basis of the prototype flight, giving about 7 days of data, a competitive limit on the ultra-high energy neutrino flux could be derived [204].

5.3. High-energy muons

Atmospheric muons, being a major background for neutrino telescopes, carry valuable information as messengers of hadronic interactions in the atmosphere. Muons are also directly linked to atmospheric neutrino production and can be used to test predictions on neutrino fluxes as needed for oscillation parameter analyses [208,209]. Particularly interesting is the comparison of muon fluxes to simulations performed with the same codes as used for air shower analyses [210,211,209,212]. Of course, muon flux predictions depend on both the used hadronic interaction model and the assumed primary cosmic ray flux.

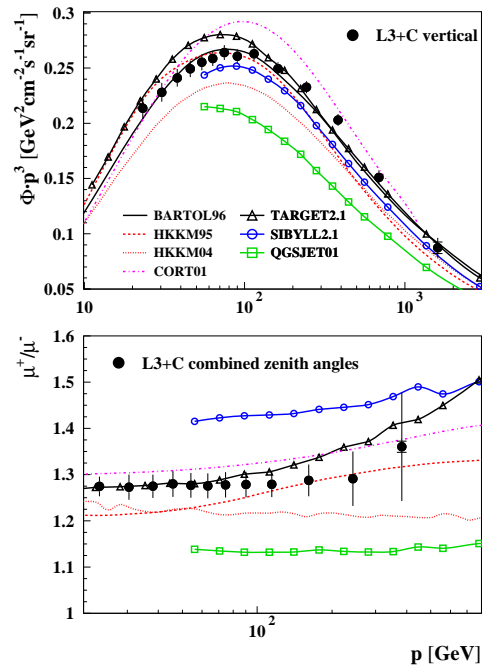


Figure 7. Vertical atmospheric muon flux as measured by L3+C. The upper panel shows the flux of all muons and the lower panel the charge ratio. The data are compared with different theoretical predictions [210,213].

Very precise high-energy muon measurements can be carried out by particle physics detectors

at colliders. For example, Fig. 7 shows the inclusive muon flux and charge ratio measured by the L3 Collab. [213]. The experimental results for vertical muons are compared to different theoretical predictions. In this case, in contrast to EAS simulations, QGSJET01 predicts a smaller muon flux than SIBYLL 2.1 (cmp. Fig. 3). Hadronic interaction models tuned for muon and neutrino flux calculations give a better description of the data [212]. As known from simulations at lower energy [209,214], the muon charge ratio is found to be very sensitive to the production of fast secondary hadrons. None of the models implemented in CORSIKA gives a good overall description of the data. The deficit of muons found relative to CORSIKA simulations is also seen by two other LEP experiments. The DELPHI and Aleph groups find that the number of high energy muon bundles cannot be described by the hadronic interaction models available in CORSIKA, assuming even a completely iron-dominated primary composition [215,216].

At higher energy, the AMANDA and NESTOR collaborations have also measured the atmospheric muon flux in the TeV energy region [62,193]. These measurements are integral flux determinations because of the very limited energy resolution of neutrino telescopes. The AMANDA Collab. have also compared their measurement to simulations with CORSIKA and find good agreement within the experimental uncertainties [62].

6. Conclusions and outlook

Flux and composition of ultra-high energy cosmic rays are still very uncertain because of the low statistics of showers observed so far and the model-dependence of the shower data interpretation. Significant progress in this field is expected by new large-aperture installations – the Pierre Auger Observatory and the Telescope Array [58]. To study the flux at even higher energies $\sim 10^{21}$ eV with sufficient statistics, new techniques will be required. Observing the atmosphere from outer space is one possible solution to increase the aperture further (for example, EUSO [148]). Another possibility could be the use of radio antenna arrays similar to that of particle

detectors [217].

The situation is similar in the knee energy region. Although the all-particle flux is known rather well there are large uncertainties in the composition. Nevertheless a clear trend from a mixed composition at low energy to a predominantly heavy one above the knee is seen in all recent measurements. The experimental errors are completely dominated by the systematic uncertainties due to our limited understanding of hadronic interactions at high energy and in forward direction.

The dependence on air shower simulations simulations can be reduced by combining different detection techniques to measure qualitatively different shower observables at the same time. Experiments of this type are the Pierre Auger Observatory, TA, and IceCube/IceTop.

Whereas there are several detectors measuring the cosmic ray flux in the knee region and at ultra-high energy, there is a lack of data in the energy range $10^{17} - 10^{19}$ eV. It is clear that the latter range is of great interest as it is expected to cover the transition from Galactic to extragalactic cosmic rays. KASCADE-Grande and IceTop will measure showers only up to $10^{17.5}$ eV with good statistics. Therefore it is worthwhile to upgrade large-aperture instruments such as Auger or TA to extend their energy range down to 10^{17} eV.

The field of emulsion chamber measurements is still full of mysteries. After more than 30 years the interpretation of one of the most famous emulsion chamber events, Centauro-I, has changed completely, now being even more difficult to explain. Not a single non-emulsion experiment could confirm any of the claimed exotic event features. Substantial progress in this field can only be expected by new measurements combining large-aperture emulsion stacks and modern particle detectors.

Many of the questions related to cosmic rays and astroparticle physics can only be solved by measuring and understanding secondary particle fluxes. There has already been enormous progress in the field of gamma-ray and neutrino measurements and much more can be expected for the next years. The second generation imaging air Cherenkov telescopes will provide high resolution

images of TeV gamma-ray sources and water/ice detectors of km³ size will probe the neutrino flux in the same energy range. Neutrino fluxes at ultra-high energy will be searched for by large-aperture air shower installations and dedicated radio signal experiments. The field of high-energy neutrino astronomy is still in an infantile stage but with a bright future ahead.

For all these measurements and related data analyses, detailed simulations are very important. Shower simulation tools in general and hadronic interaction models in particular should be improved continuously and tested by comparing them with a large variety of data. During the last decade great progress was achieved by the introduction of multi-purpose code packages such as CORSIKA and AIRES that are professionally maintained. However, it should not be overlooked that the quality of air shower and inclusive flux simulations depends crucially on particle production data measured in fixed-target and collider experiments. At the moment the lack of suitable accelerator data is the dominant source of systematic uncertainties in cosmic ray measurements. As we don't have a calculable theory of hadronic multiparticle production, there is no change of this dependence on accelerator data to be expected in near future.

Acknowledgements

It is the author's pleasure to thank the organizers for inviting him to participate in this very interesting and fruitful symposium. He gratefully acknowledges clarifying and illuminating discussions with many participants of this meeting and his colleagues from the KASCADE-Grande and Pierre Auger collaborations. In particular he benefited from discussions with K. Belov, V. Berezhinsky, A. Haungs, D. Heck, S. Ostapchenko, T. Pierog, L. Resvanis, H. Ulrich, M. Unger, A. Watson, and S. Westerhoff. The author also would like to thank D. Heck for providing him Figs. 3 and 4.

REFERENCES

1. L. Anchordoqui, T. Paul, S. Reucroft, and J. Swain, *Int. J. Mod. Phys. A*18 (2003) 2229–2366 and hep-ph/0206072.
2. A. Haungs, H. Rebel, and M. Roth, *Rept. Prog. Phys.* 66 (2003) 1145–1206.
3. A. A. Watson, astro-ph/0312475.
4. J. W. Cronin, astro-ph/0402487.
5. R. Engel and H. Klages, *Comptes Rendus Physique* 5 (2004) 505–518.
6. M. Takeda *et al.* (AGASA Collab.), Prepared for 28th International Cosmic Ray Conference (ICRC 2003), Tsukuba, Japan, 31 Jul - 7 Aug 2003, p. 381.
7. K. Shinozaki (AGASA Collab.), these proceedings.
8. M. Nagano *et al.*, *J. Phys. G*10 (1984) 1295.
9. M. Nagano *et al.*, *J. Phys. G*18 (1992) 423–442.
10. S. Westerhoff (HiRes Collab.), these proceedings.
11. R. U. Abbasi *et al.* (HiRes Collab.), *Phys. Rev. Lett.* 92 (2004) 151101 and astro-ph/0208243.
12. T. Abu-Zayyad *et al.* (HiRes Collab.), astro-ph/0208301.
13. T. Abu-Zayyad *et al.* (HiRes-MIA Collab.), *Astrophys. J.* 557 (2001) 686–699 and astro-ph/0010652.
14. A. Haungs (KASCADE Collab.), these proceedings, astro-ph/0412610.
15. H. Ulrich *et al.*, *Eur. Phys. J. C*33 (2004) s944–s946.
16. Y. A. Fomin *et al.*, Prepared for 28th International Cosmic Ray Conference (ICRC 2003), Tsukuba, Japan, 31 Jul - 7 Aug 2003, p. 119-122.
17. T. Shibata (RUNJOB Collab.), these proceedings.
18. M. Furukawa *et al.* (RUNJOB Collab.), Prepared for 28th International Cosmic Ray Conference (ICRC 2003), Tsukuba, Japan, 31 Jul - 7 Aug 2003, p. 1885-1888.
19. H. S. Ahn *et al.* (ATIC-1 Collab.), Prepared for 28th International Cosmic Ray Conference (ICRC 2003), Tsukuba, Japan, 31 Jul - 7 Aug 2003 p. 1833-1836.
20. G. Navarra (EAS-TOP Collab.), these proceedings.
21. M. Aglietta *et al.* (EAS-TOP Collab.), *Astropart. Phys.* 10 (1999) 1–9.
22. Y. Q. Ma (Tibet AS γ Collab.), these proceedings.
23. M. Amenomori *et al.* (Tibet AS γ Collab.), Prepared for 28th International Cosmic Ray Conference (ICRC 2003), Tsukuba, Japan, 31 Jul - 7 Aug 2003, p. 143-146.
24. G. Zatsepin, these proceedings.
25. M. Takeda *et al.* (AGASA Collab.), *Phys. Rev. Lett.* 81 (1998) 1163–1166 and astro-ph/9807193.
26. D. De Marco, P. Blasi, and A. V. Olinto,

- Astropart. Phys. 20 (2003) 53–65 and astro-ph/0301497.
27. M. Takeda *et al.* (AGASA Collab.), Astropart. Phys. 19 (2003) 447–462 and astro-ph/0209422.
 28. D. R. Bergman *et al.* (HiRes Collab.), Prepared for 28th International Cosmic Ray Conference (ICRC 2003), Tsukuba, Japan, 31 Jul - 7 Aug 2003, p. 397.
 29. S. P. Knurenko (Yakutsk Collab.), these proceedings, astro-ph/0411484.
 30. N. N. Kalmykov and S. S. Ostapchenko, Phys. At. Nucl. 56 (1993) (3) 346.
 31. N. N. Kalmykov, S. Ostapchenko, and A. I. Pavlov, Nucl. Phys. B (Proc. Suppl.) 52B (1997) 17.
 32. R. U. Abbasi *et al.* (HiRes Collab.), Astrophys. J. 622 (2005) 910–926 and astro-ph/0407622.
 33. K. Shinozaki and M. Teshima (AGASA Collab.), Nucl. Phys. Proc. Suppl. 136 (2004) 18–27.
 34. S. P. Knurenko (Yakutsk Collab.), these proceedings, astro-ph/0411483.
 35. D. R. Bergman (HiRes Collab.), Mod. Phys. Lett. A18 (2003) 1235–1245 and hep-ex/0307059.
 36. V. Berezhinsky, A. Z. Gazizov, and S. I. Grigorieva, astro-ph/0502550.
 37. H. J. Drescher, these proceedings, astro-ph/0411143.
 38. S. Ostapchenko, these proceedings, astro-ph/0412591.
 39. T. Pierog, these proceedings, astro-ph/0411260.
 40. R. S. Fletcher, T. K. Gaisser, P. Lipari, and T. Stanev, Phys. Rev. D50 (1994) 5710.
 41. R. Engel, T. K. Gaisser, P. Lipari, and T. Stanev, in Proceedings of the 26th International Cosmic Ray Conference (Salt Lake City) vol. 1, p. 415, 1999.
 42. H. J. Drescher, M. Hladik, S. Ostapchenko, T. Pierog, and K. Werner, Phys. Rept. 350 (2001) 93–289 and hep-ph/0007198.
 43. A. A. Watson, these proceedings, astro-ph/0410514.
 44. M. Ave, J. Knapp, M. Marchesini, M. Roth, and A. A. Watson, Prepared for 28th International Cosmic Ray Conference (ICRC 2003), Tsukuba, Japan, 31 Jul - 7 Aug 2003, p. 349.
 45. M. T. Dova, M. E. Mancenido, A. G. Mariazzi, T. P. McCauley, and A. A. Watson, Astropart. Phys. 21 (2004) 597–607.
 46. P. Homola, these proceedings, astro-ph/0411060.
 47. M. Risse *et al.*, astro-ph/0502418.
 48. M. Teshima *et al.* (AGASA Collab.), Prepared for 28th International Cosmic Ray Conference (ICRC 2003), Tsukuba, Japan, 31 Jul - 7 Aug 2003, p. 437.
 49. C. B. Finley and S. Westerhoff, Astropart. Phys. 21 (2004) 359–367 and astro-ph/0309159.
 50. T. Stanev, P. L. Biermann, J. Lloyd-Evans, J. P. Rachen, and A. Watson, Phys. Rev. Lett. 75 (1995) 3056–3059 and astro-ph/9505093.
 51. P. G. Tinyakov and I. I. Tkachev, JETP Lett. 74 (2001) 445–448 and astro-ph/0102476.
 52. D. S. Gorbunov, P. G. Tinyakov, I. I. Tkachev, and S. V. Troitsky, Astrophys. J. 577 (2002) L93 and astro-ph/0204360.
 53. P. G. Tinyakov and I. I. Tkachev, Astropart. Phys. 18 (2002) 165–172 and astro-ph/0111305.
 54. D. S. Gorbunov, P. G. Tinyakov, I. I. Tkachev, and S. V. Troitsky, JETP Lett. 80 (2004) 145–148 and astro-ph/0406654.
 55. K. H. Kampert (Auger Collab.), these proceedings, astro-ph/0501074.
 56. <http://www.auger.org>.
 57. M. Fukushima, Prog. Theor. Phys. Suppl. 151 (2003) 206–210.
 58. http://www-ta.icrr.u-tokyo.ac.jp/TA_Proposal/.
 59. J. Abraham *et al.* (Auger Collab.), Nucl. Instrum. Meth. A523 (2004) 50–95.
 60. J. R. Hoerandel, Astropart. Phys. 21 (2004) 241–265 and astro-ph/0402356.
 61. S. P. Swordy *et al.*, Astropart. Phys. 18 (2002) 129–150 and astro-ph/0202159.
 62. A. Karle (AMANDA Collab.), these proceedings.
 63. A. A. Petrukhin, these proceedings.
 64. T. Antoni *et al.* (KASCADE Collab.), Astropart. Phys. 16 (2002) 373–386.
 65. T. Antoni *et al.* (KASCADE Collab.), Nucl. Instrum. Meth. A513 (2003) 490–510.
 66. M. Aglietta *et al.* (MACRO Collab.), Astropart. Phys. 20 (2004) 641–652 and astro-ph/0305325.
 67. J. Ahrens *et al.* (AMANDA and SPASE Collab.), Astropart. Phys. 21 (2004) 565–581.
 68. M. Amenomori *et al.* (Tibet AS γ Collab.), Prepared for 28th International Cosmic Ray Conference (ICRC 2003), Tsukuba, Japan, 31 Jul - 7 Aug 2003, p. 107–110.
 69. D. Heck, J. Knapp, J. Capdevielle, G. Schatz, and T. Thouw, in Wissenschaftliche Berichte FZKA 6019, Forschungszentrum Karlsruhe, 1998.
 70. K. Asakimori *et al.* (JACEE Collab.), Astrophys. J. 502 (1998) 278–283.
 71. H. S. Ahn *et al.* (ATIC-2 Collab.), Prepared for 28th International Cosmic Ray Conference (ICRC 2003), Tsukuba, Japan, 31 Jul - 7 Aug 2003, 1853–1856.

72. J. Candia, S. Mollerach, and E. Roulet, JCAP 0305 (2003) 003 and astro-ph/0302082.
73. T. Antoni *et al.* (KASCADE Collab.), Astrophys. J. 604 (2004) 687–692 and astro-ph/0312375.
74. T. Antoni *et al.* (KASCADE Collab.), Astrophys. J. 608 (2004) 865–871 and astro-ph/0402656.
75. M. Amenomori *et al.* (Tibet AS γ Collab.), Phys. Rev. Lett. 93 (2004) 061101 and astro-ph/0408187.
76. M. Aglietta *et al.* (EAS-TOP Collab.), Astrophys. J. 470 (1996) 501–505.
77. T. Antoni *et al.* (KASCADE Collab.), Astropart. Phys. 16 (2002) 245–263 and astro-ph/0102443.
78. J. Knapp, D. Heck, and G. Schatz, in Wissenschaftliche Berichte FZKA 5828, Forschungszentrum Karlsruhe, 1996.
79. J. Knapp, D. Heck, S. J. Sciutto, M. T. Dova, and M. Risse, Astropart. Phys. 19 (2003) 77–99 and astro-ph/0206414.
80. R. Engel, T. K. Gaisser, and T. Stanev, Proc. of XXIX Int. Symposium on Multiparticle Dynamics, Brown University, USA, Aug. 8-13, p. 457, 2000.
81. H.-J. Drescher and G. R. Farrar, Astropart. Phys. 19 (2003) 235–244 and hep-ph/0206112.
82. D. Heck *et al.*, Prepared for 28th International Cosmic Ray Conference (ICRC 2003), Tsukuba, Japan, 31 Jul - 7 Aug 2003, p. 279.
83. K. Hänflgen and J. Ranft, Comp. Phys. Commun. 39 (1986) 37.
84. A. Mücke, R. Engel, R. J. Protheroe, J. P. Rachen, and T. Stanev, Comp. Phys. Commun. 124 (2000) 290.
85. A. Fasso, A. Ferrari, J. Ranft, and R. P. Sala, in Proc. of Int. Conf. on Advanced Monte Carlo for Radiation Physics, Particle Transport Simulation and Applications (MC 2000), Lisbon, Portugal, 23-26 Oct 2000, A. Kling, F. Barao, M. Nakagawa, L. Tavora, P. Vaz eds., Springer-Verlag Berlin, p. 955, 2001.
86. J. Ranft, Phys. Rev. D51 (1995) 64.
87. D. Heck and S. Ostapchenko, private communication.
88. R. Engel, Nucl. Phys. B (Proc. Suppl.) 122 (2003) 40.
89. J. Alvarez-Muniz, R. Engel, T. K. Gaisser, J. A. Ortiz, and T. Stanev, Phys. Rev. D66 (2002) 033011 and astro-ph/0205302.
90. S. S. Ostapchenko, J. Phys. G29 (2003) 831–842.
91. T. Stanev, these proceedings.
92. V. N. Gribov, M. L. Levin, and M. G. Ryskin, Phys. Rep. 100 (1983) 1.
93. A. H. Mueller, hep-ph/0501012.
94. talks at Workshop “QCD at Cosmic Energies”, Aug 29 - Sep 5, 2004, Erice, Italy, <http://www.lpthe.jussieu.fr/Erice/>, the next workshop will be held 2005 in Greece, see <http://www.lpthe.jussieu.fr/Greece/>.
95. E. Iancu and R. Venugopalan, hep-ph/0303204.
96. K. Golec-Biernat and M. Wusthoff, Phys. Rev. D59 (1999) 014017 and hep-ph/9807513.
97. J. R. Forshaw, R. Sandapen, and G. Shaw, Int. J. Mod. Phys. A19 (2004) 5425–5432 and hep-ph/0407261.
98. H. Abramowicz and A. Caldwell, Rev. Mod. Phys. 71 (1999) 1275.
99. S. Lange, these proceedings.
100. E. Levin, hep-ph/0408039.
101. P. A. Steinberg, Acta Phys. Polon. B35 (2004) 235–239.
102. A. B. Kaidalov and K. A. Ter-Martirosian, Sov. J. Nucl. Phys. 39 (1984) 979.
103. S. Ostapchenko, these proceedings, astro-ph/0412332.
104. A. B. Kaidalov, L. A. Ponomarev, and K. A. Ter-Martirosyan, Sov. J. Nucl. Phys. 44 (1986) 468.
105. R. Luna, A. Zepeda, C. A. Garcia Canal, and S. J. Sciutto, Phys. Rev. D70 (2004) 114034 and hep-ph/0408303.
106. R. Engel, Nucl. Phys. Proc. Suppl. 122 (2003) 437–446 and hep-ph/0212340.
107. D. Heck, private communication.
108. P. Rapidis, these proceedings.
109. M. Albrow, L. Nodulman, and P. Giromini, CDF/PUBLIC/4844, available from CDF web page, 1999.
110. M. Zha, J. Knapp, and S. Ostapchenko, Prepared for 28th International Cosmic Ray Conference (ICRC 2003), Tsukuba, Japan, 31 Jul - 7 Aug 2003, p. 515-518.
111. R. Orava, these proceedings.
112. V. Avati *et al.* (TOTEM Collab.), Eur. Phys. J. C34 (2004) s255–s268.
113. R. Engel, Nucl. Phys. B (Proc. Suppl.) 75A (1999) 62 and astro-ph/9811225.
114. L. Frankfurt, W. Koepf, and M. Strikman, Phys. Lett. B405 (1997) 367–372 and hep-ph/9702236.
115. H. J. Drescher, A. Dumitru, and M. Strikman, hep-ph/0408073.
116. H. J. Drescher, A. Dumitru, and M. Strikman, hep-ph/0501165.
117. J. T. Mitchell (NA35 Collab.), Nucl. Phys. A566 (1994) 415c–418c.
118. F. Videbaek, Heavy Ion Phys. 15 (2002) 303–313

- and nucl-ex/0106017.
- 119.A. Capella and B. Z. Kopeliovich, Phys. Lett. B381 (1996) 325–330 and hep-ph/9603279.
- 120.A. Capella, Phys. Lett. B542 (2002) 65–70.
- 121.K. Itakura, Y. V. Kovchegov, L. McLerran, and D. Teaney, Nucl. Phys. A730 (2004) 160–190 and hep-ph/0305332.
- 122.H. Fesefeldt, RWTH Aachen, 1985.
- 123.A. M. Hillas, in Proc. 17th Int. Cosmic Ray Conf. 8, p. 193, Paris, France, 1981.
- 124.A. M. Hillas, in Proc. 24th Int. Cosmic Ray Conf. 1, p. 270, Rome, Italy, 1995.
- 125.S. J. Sciutto, astro-ph/9911331.
- 126.H.-J. Drescher, M. Bleicher, S. Soff, and H. Stoecker, Astropart. Phys. 21 (2004) 87–94 and astro-ph/0307453.
- 127.D. Heck, private communication, astro-ph/0410735.
- 128.M. Bleicher *et al.*, J. Phys. G: Nucl. Part. Phys. 25 (1999) 1859.
- 129.R. Engel, T. K. Gaisser, and T. Stanev, Phys. Lett. B472 (2000) 113–118 and hep-ph/9911394.
- 130.G. Barr and R. Engel, these proceedings, astro-ph/0404356.
- 131.J. J. Gomez-Cadenas (HARP Collab.), Nucl. Phys. Proc. Suppl. 143 (2005) 291–296 and hep-ex/0410043.
- 132.R. Raja, hep-ex/0501005, 2005.
- 133.J. Alvarez-Muniz, R. Engel, T. K. Gaisser, J. A. Ortiz, and T. Stanev, Phys. Rev. D69 (2004) 103003 and astro-ph/0402092.
- 134.K. Belov (HiRes Collab.), Prepared for 28th International Cosmic Ray Conference (ICRC 2003), Tsukuba, Japan, 31 Jul - 7 Aug 2003, p. 1567–1570.
- 135.K. Belov (HiRes Collab.), these proceedings.
- 136.J. Zabierowski (KASCADE Collab.), these proceedings.
- 137.J. Milke (KASCADE Collab.), these proceedings.
- 138.A. Haungs, these proceedings.
- 139.A. Haungs and J. Kempa, Nuovo Cim. 26C (2003) 503–520.
- 140.J. R. Hoerandel, these proceedings.
- 141.J. R. Hoerandel, J. Phys. G29 (2003) 2439–2464 and astro-ph/0309010.
- 142.H. J. Drescher, these proceedings, astro-ph/0411144.
- 143.L. G. Dedenko, these proceedings.
- 144.G. Bossard *et al.*, Phys. Rev. D63 (2001) 054030 and hep-ph/0009119.
- 145.H.-J. Drescher and G. R. Farrar, Phys. Rev. D67 (2003) 116001 and astro-ph/0212018.
- 146.J. A. Ortiz, G. A. Medina Tanco, and V. de Souza, astro-ph/0411421.
- 147.T. Pierog, H. J. Drescher, F. Liu, S. Ostapchenko, and K. Werner, Nucl. Phys. A715 (2003) 895–898 and hep-ph/0211202.
- 148.P. Gorodetzky (EUSO Collab.), these proceedings, astro-ph/0502187.
- 149.C. M. G. Lattes, Y. Fujimoto, and S. Hasegawa, Phys. Rept. 65 (1980) 151.
- 150.S. A. Slavatsky, Nucl. Phys. Proc. Suppl. 122 (2003) 3–11.
- 151.M. Tamada, these proceedings.
- 152.J. Milke (KASCADE Collab.), these proceedings.
- 153.C. M. G. Lattes *et al.* (Brazil-Japan Collab.), Prepared for 13th International Cosmic Ray Conference (ICRC 1973), Denver, CO, 17 - 30 Aug 1973, vol. 3, p. 2227; vol. 4, p. 2671.
- 154.E. Gładysz-Dziadus, Phys. Part. Nucl. 34 (2003) 285–347 and hep-ph/0111163.
- 155.Z. Włodarczyk, these proceedings, hep-ph/0410064.
- 156.M. Rybczynski, Z. Włodarczyk, and G. Wilk, Acta Phys. Polon. B33 (2002) 277–296 and hep-ph/0109225.
- 157.J. D. Bjorken and L. D. McLerran, Phys. Rev. D20 (1979) 2353.
- 158.J. D. Bjorken, Int. J. Mod. Phys. A7 (1992) 4189–4258.
- 159.T. N. Tomaras, these proceedings, hep-ph/0411081.
- 160.A. Mironov, A. Morozov, and T. N. Tomaras, hep-ph/0311318.
- 161.R. Attallah and J. N. Capdevielle, J. Phys. G19 (1993) 1381–1392.
- 162.A. Ohsawa, E. H. Shibuya, and M. Tamada, Phys. Rev. D70 (2004) 074028.
- 163.A. S. Borisov, V. M. Maksimenko, R. A. Mukhamedshin, V. S. Puchkov, and S. A. Slavatsky, Prepared for 28th International Cosmic Ray Conference (ICRC 2003), Tsukuba, Japan, 31 Jul - 7 Aug 2003, p. 85–88.
- 164.V. V. Kopenkin, A. K. Managadze, I. V. Rakobolskaya, and T. M. Roganova, Phys. Rev. D52 (1995) 2766–2774 and hep-ph/9408247.
- 165.J. N. Capdevielle, R. Attallah, and M. C. Talai, Prepared for 27th International Cosmic Ray Conference (ICRC 2001), Hamburg, Germany, 7–15 Aug 2001, p. 1410–1413.
- 166.V. I. Galkin *et al.*, Prepared for 27th International Cosmic Ray Conference (ICRC 2001), Hamburg, Germany, 7–15 Aug 2001, p. 1407–1409.

167. T. Antoni *et al.* (KASCADE Collab.), Phys. Rev. D71 (2005) 072002 and hep-ph/0503218.
168. F. Halzen and D. A. Morris, Phys. Rev. D42 (1990) 1435–1439.
169. A. De Rújula, these proceedings, astro-ph/0412094.
170. E. Waxman, these proceedings, astro-ph/0412554.
171. V. Berezhinsky, these proceedings.
172. H. Kubo *et al.* (CANGAROO Collab.), New Astron. Rev. 48 (2004) 323–329.
173. D. Horns, these proceedings.
174. J. A. Hinton (HESS Collab.), New Astron. Rev. 48 (2004) 331–337 and astro-ph/0403052.
175. E. Fernández, these proceedings.
176. D. Bastieri *et al.* (MAGIC Collab.), astro-ph/0503534.
177. F. Krennrich *et al.*, New Astron. Rev. 48 (2004) 345–349.
178. F. Aharonian *et al.* (HESS Collab.), astro-ph/0408145.
179. F. A. Aharonian *et al.* (HESS Collab.), Nature. 432 (2004) 75–77 and astro-ph/0411533.
180. K. Tsuchiya *et al.* (CANGAROO-II Collab.), Astrophys. J. 606 (2004) L115–L118 and astro-ph/0403592.
181. R. Enomoto *et al.*, Nature 416 (2002) 823–826.
182. M. Amenomori *et al.* (Tibet AS γ Collab.), Prepared for 28th International Cosmic Ray Conference (ICRC 2003), Tsukuba, Japan, 31 Jul - 7 Aug 2003, p. 3019-3022.
183. J. Goodman (Milagro Collab.), these proceedings.
184. G. Sinnis (Milagro Collab.), Prepared for 28th International Cosmic Ray Conference (ICRC 2003), Tsukuba, Japan, 31 Jul - 7 Aug 2003, p. 2583-2586.
185. R. Atkins *et al.*, Astrophys. J. 608 (2004) 680–685 and astro-ph/0403097.
186. M. Amenomori *et al.* (Tibet AS γ Collab.), astro-ph/0502039.
187. A. Atkins *et al.* (Milagro Collab.), astro-ph/0502303.
188. P. M. Saz Parkinson (Milagro Collab.), astro-ph/0503244.
189. F. Aharonian *et al.* (HEGRA Collab.), astro-ph/0501667.
190. N. Hayashida *et al.* (AGASA Collab.), Astropart. Phys. 10 (1999) 303–311 and astro-ph/9807045.
191. T. K. Gaisser, F. Halzen, and T. Stanev, Phys. Rept. 258 (1995) 173–236 and hep-ph/9410384.
192. E. Andres *et al.* (AMANDA Collab.), Astropart. Phys. 13 (2000) 1–20 and astro-ph/9906203.
193. S. Tzamarias, these proceedings.
194. C. Spiering *et al.* (BAIKAL Collab.), astro-ph/0404096.
195. V. S. Berezhinsky and A. Y. Smirnov, Astrop. Sp. Sci. 32 (1975) 461.
196. E. Waxman and J. N. Bahcall, Phys. Rev. D59 (1999) 023002 and hep-ph/9807282.
197. K. Mannheim, R. J. Protheroe, and J. P. Rachen, Phys. Rev. D63 (2001) 023003 and astro-ph/9812398.
198. D. Nygren (IceCube Collab.), these proceedings.
199. J. Ahrens *et al.* (IceCube Collab.), Astropart. Phys. 20 (2004) 507–532 and astro-ph/0305196.
200. I. Sokalski (ANTARES Collab.), hep-ex/0501003.
201. A. G. Tsirigotis (NESTOR Collab.), Eur. Phys. J. C33 (2004) s956–s958.
202. E. Migneco *et al.*, To appear in the proceedings of 21st International Conference on Neutrino Physics and Astrophysics (Neutrino 2004), Paris, France, 14-19 Jun 2004.
203. <http://km3net.org>.
204. J. Learned, these proceedings.
205. N. G. Lehtinen, P. W. Gorham, A. R. Jacobson, and R. A. Roussel-Dupre, Phys. Rev. D69 (2004) 013008 and astro-ph/0309656.
206. P. W. Gorham *et al.*, Phys. Rev. Lett. 93 (2004) 041101 and astro-ph/0310232.
207. P. Miocinovic *et al.*, astro-ph/0503304.
208. T. K. Gaisser and M. Honda, Ann. Rev. Nucl. Part. Sci. 52 (2002) 153–199 and hep-ph/0203272.
209. I. Brancus, these proceedings.
210. P. Le Coultre (L3 Collab.), these proceedings.
211. J. Ridky, these proceedings.
212. Y. Q. Ma, these proceedings.
213. P. Achard *et al.* (L3 Collab.), Phys. Lett. B598 (2004) 15–32 and hep-ex/0408114.
214. J. Wentz *et al.*, Phys. Rev. D67 (2003) 073020 and hep-ph/0301199.
215. J. Ridky and P. Travnicek (DELPHI Collab.), Nucl. Phys. Proc. Suppl. 138 (2005) 295–298.
216. V. Avati *et al.*, Astropart. Phys. 19 (2003) 513–523.
217. H. Falcke, P. Gorham, and R. J. Protheroe, New Astron. Rev. 48 (2004) 1487–1510 and astro-ph/0409229.